

Spatial variation of seismic *b*-values beneath Makushin Volcano, Unalaska Island, Alaska

David L. Bridges*, Stephen S. Gao

Department of Geology, Kansas State University, Manhattan, KS 66506, USA

Received 21 December 2005; received in revised form 24 February 2006; accepted 6 March 2006

Available online 19 April 2006

Editor: S. King

Abstract

The frequency-magnitude distribution was spatially mapped beneath Makushin Volcano, Unalaska Island, Alaska using an earthquake catalog of 491 events that occurred between July 2001 and April 2005. An area of high seismic *b*-values (~ 2.0) is found ~ 4 km east of Makushin's main vent at a depth between 4 and 7 km. The anomaly is statistically significant based on Utsu's *p*-test [T. Utsu, On seismicity, in Report of the Joint Research Institute for Statistical Mathematics, Tokyo (1992) 139–157], and is not data processing method or parameter dependent. Interestingly, a recent InSAR interferometric study [Z. Lu, J.A. Power, V.S. McConnell, C. Wicks Jr., D. Dzuris, Preeruptive inflation and surface interferometric coherence characteristics by satellite radar interferometry at Makushin volcano, Alaska: 1993–2000, *J. Geophys. Res.* 107 (2002) 2266, doi:10.1029/2001JB000970] inferred a surface uplift of about 7 cm during the two-year period prior to October 1995, centered approximately in the area with the observed anomalous *b*-values. The uplift was caused by the volume increase of an inferred magma chamber at a depth of about 7 km. The close correspondence of the seismic and InSAR observations suggests that the heterogeneous area associated with the observed high *b*-values is most likely the result of increased crack density associated with the magma chamber. This study demonstrates the effectiveness of combining InSAR and seismological observations in locating magma chambers and areas of high heterogeneity in the crust.

© 2006 Elsevier B.V. All rights reserved.

Keywords: seismic *b*-value; magma chamber; Makushin Volcano; Aleutian Arc; Alaska

1. Introduction

Makushin is a 2036 m high stratovolcano located on Unalaska Island, Alaska (Fig. 1). The volcano is located 28 km west of the largest population center of the Aleutians, Unalaska/Dutch Harbor [1]. It is one of many active volcanic centers located along the extensive

Aleutian Arc. Makushin's last confirmed eruption was a small explosive one in 1995 with the last significant eruption occurring in 1826 [2]. Makushin has had several small steam and ash emissions since its discovery. Little is known about the magma distribution in the crust beneath Makushin. The purpose of the study is to provide constraints on the 3-D distribution of magma chamber(s) beneath the active volcano by mapping the seismic *b*-value. We use results from a recent InSAR study [3] for the interpretation of the seismic observations.

* Corresponding author.

E-mail addresses: dbridges@ksu.edu (D.L. Bridges), gao@ksu.edu (S.S. Gao).

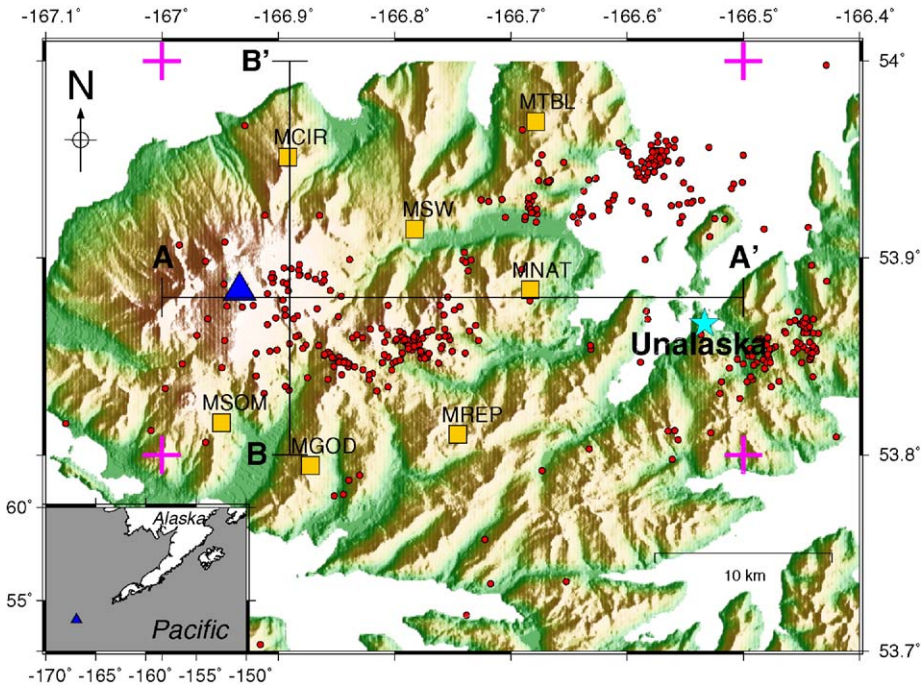


Fig. 1. Map of Makushin Volcano and surrounding area. The blue triangle shows the location of Makushin's main vent. Squares mark the locations of seismic stations, and filled circles are the epicenters of the earthquakes used in the study. The blue star marks the location of Unalaska/Dutch Harbor. The crosses outline the area that was spatially mapped using b -values. A–A' and B–B' are the locations of the cross-sections in Fig. 4. The inset shows Makushin's geographic relationship to the western part of Alaska.

The frequency–magnitude distribution (FMD) was first introduced in Japan by Ishimoto and Iida [4], and subsequently in the United States by Gutenberg and Richter [5]. The FMD equation is commonly written as

$$\log N = a - bM, \quad (1)$$

where N is the cumulative number of earthquakes with magnitude equal to or greater than M , a is a constant describing the seismic productivity of the area studied, and b is another constant quantifying the slope of the FMD. The constants a and b are dependent on factors such as applied shear stress and material heterogeneity [6,7]. b -values less than 1 indicate areas of crustal homogeneity and high stress, and values greater than 1 indicate crustal heterogeneity and low stress. Typical b -values range from 0.6 to 1.4 with a global mean of about 1.0 [8]. In volcanic areas, however, b -values can be as high as 3.0 [9–11].

As summarized in a recent review article [12], spatial and temporal mapping of b -values has found applications to many geologic problems, including the determination of the magma chamber location, size, and morphology [9,11,13–18]. Such a determination can greatly aid the study of a volcano's evolution and the

mitigation of its hazards. In addition to mapping b -values, a number of other methods have been used to infer crustal melt location such as seismic body-wave tomography [19,20], radar interferometry [3], and other geodetic techniques [21,22].

So far b -values have been mapped at 13+ volcanoes, and virtually all of them show high b anomalies in the top 7 km in the area surrounding the magma bodies [11]. The high b -value regions have been attributed to crustal heterogeneity [6], high thermal gradients [23], and high pore pressure found in the vicinity of a magma chamber, all of which lower effective stress [12,24]. Sanchez et al. [13] suggest processes such as vesiculation and fragmentation of ascending magma may increase the b -value in upper magmatic conduits by creating stress-induced fractures. A recent review paper by McNutt [11] indicated that nearly half of the 13 volcanoes mapped using b -values show a significantly high b -value region in the depth of 3–4 km relative to the regions above and below. This is primarily due to the exsolution of gases at this depth and the existence of open cracks [11].

Note that while anomalously high b -values are used to infer pockets of crust with a high degree of partial melting, magma chambers have no associated b -value, because magma does not have enough internal shear to

generate earthquakes. Consequently, the detected high b -values are in the area surrounding and affected by the magma chamber.

2. Data

Makushin was instrumented in July 1996 with five Mark Products L4 seismometers and a Mark Products L22 seismometer (Fig. 1). On January 1, 2002, station MREP was added which resulted in a total of seven instruments in the Makushin subnet [25]. The subnet is an event-triggered system. The earthquakes were located using HYPOELLIPE, a program that finds the hypocenter, magnitude, and focal mechanism of an event [26]. The average vertical and horizontal error for the Makushin data set is 3.5 and 2.6 km, respectively, and the average RMS error is 0.117 s [25,27]. Events without magnitude, with fewer than three P -phases, with less than one S -phase, or with standard hypocentral errors greater than 15 km were removed from the catalog [28,29].

The Alaska Volcano Observatory (AVO) located a total of 1272 events using data recorded by the Makushin subnet with a temporal range from July 1996 to April 2005. We next determine the magnitude of completeness, M_c , of the catalog. So far, a number of approaches have been proposed to compute M_c [12,30–32] (see [33] for a comparative study). Based on the nature of our study area and the characteristics of our catalog, the procedure of Wiemer and Wyss [12] is used in the study. Our algorithm first calculates the mean magnitude of the data set. Next the events are placed in bins of similar magnitude. The default magnitude values for the creation of a synthetic FMD are 0 to 5 with a 0.1 magnitude interval. The algorithm creates a synthetic FMD. The following equation is used to compare the synthetic FMD and the observed one until a best fit is observed:

$$R(a, b, M_i) = 100 - \frac{\sum_{i=M_i}^{M_{\max}} |B_i - S_i|}{\sum_i B_i} 100, \quad (2)$$

where B_i is the observed cumulative number of events per magnitude, S_i is the predicted cumulative number of events, R is the absolute difference or goodness of fit, a and b are from Eq. (1), and M_i is the minimum magnitude.

Wiemer and Wyss [12] define the 90% goodness of fit level as M_c , which implies that 90% of the variability in the observed FMD can be described with the FMD power law. Volcanic catalogs, however, rarely reach this level mainly due to the relatively small number of

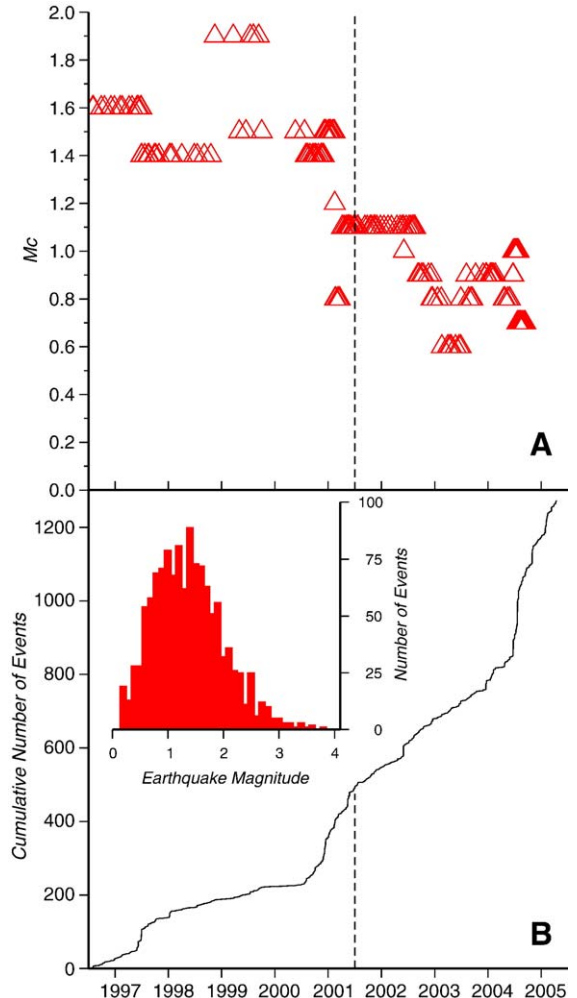


Fig. 2. A) M_c as a function of time. The catalog used in the study consists of events after the dashed line. A moving window of 100 events was used to calculate M_c , using a 5 event increment. B) Cumulative number of earthquakes in the original catalog. The final data set consists of all events right of the dashed line. Inset shows the number of events placed in 0.1 magnitude bins.

events and sometimes a bimodal distribution (nonlinearity) caused by earthquake swarms. The best goodness of fit that could be achieved with our catalog is 74%, corresponding to a M_c of ~ 1.25 for the complete 1272 event catalog, which is similar to the value (1.2) determined by Dixon et al. [25].

Similar to most seismic networks [32], our calculated M_c shows significant temporal variations (Fig. 2). In particular, a dramatic decrease in M_c is found near June 2001, from about 1.5 to 1.1. The sharp contrast in M_c before and after July 1, 2001 is significant enough for us to reject events before July 2001 in favor of the part of the catalog that is more complete. After removing events with no depth determination, a catalog consisting of 491

events with magnitude $\geq M_c$ occurred after June 2001 was compiled. M_c varied spatially from 0.9 to 1.2 for the post June 2001 catalog when mapped using the approach similar to the one used by Wiemer and Wyss [32].

The magnitude of the 491 events used in the study ranges from 0.9 to 3.1, with a mean of 1.4 ± 0.4 . The events are mostly clustered in three groups (Fig. 1). The first group is under Makushin's east flank, the second is located under Unalaska Bay, and the third group is directly west of Unalaska/Dutch Harbor. On average earthquakes in the first group are about 3 km shallower than those in the other two groups (~ 5 vs. 8 km).

3. Method

b -values were mapped using a grid technique [34] in which nodes were created 1 km apart horizontally and 1 km apart in depth. The number of nodes for the study area along the NS, EW, and vertical directions is 25, 33,

and 14, respectively. Because it is well known that M_c varies spatially [32], it was calculated at each node to maximize the accuracy of the b -value.

A constant N of 50 events was sampled within a sphere centered at each node. For areas with expected large spatial variations in b -values such as beneath active volcanoes, $N=50$ is thought to be sufficient to obtain statistically significant results [12]. Indeed, $N=50$ was used to map b -value distribution within a $10 \times 10 \times 20$ km area based on 450 events in the vicinity of Mt. Etna, Italy [17]. For each node, the volume of the sampling sphere is inversely proportional to the density of earthquake hypocenters in the vicinity of the node. The radius of the sphere is not allowed to extend beyond 8 km, because events further than 8 km away from the node are not considered to be local and therefore are not indicative of the b -value at a given node. If less than 50 events were located within 8 km of the node, the node was not mapped.

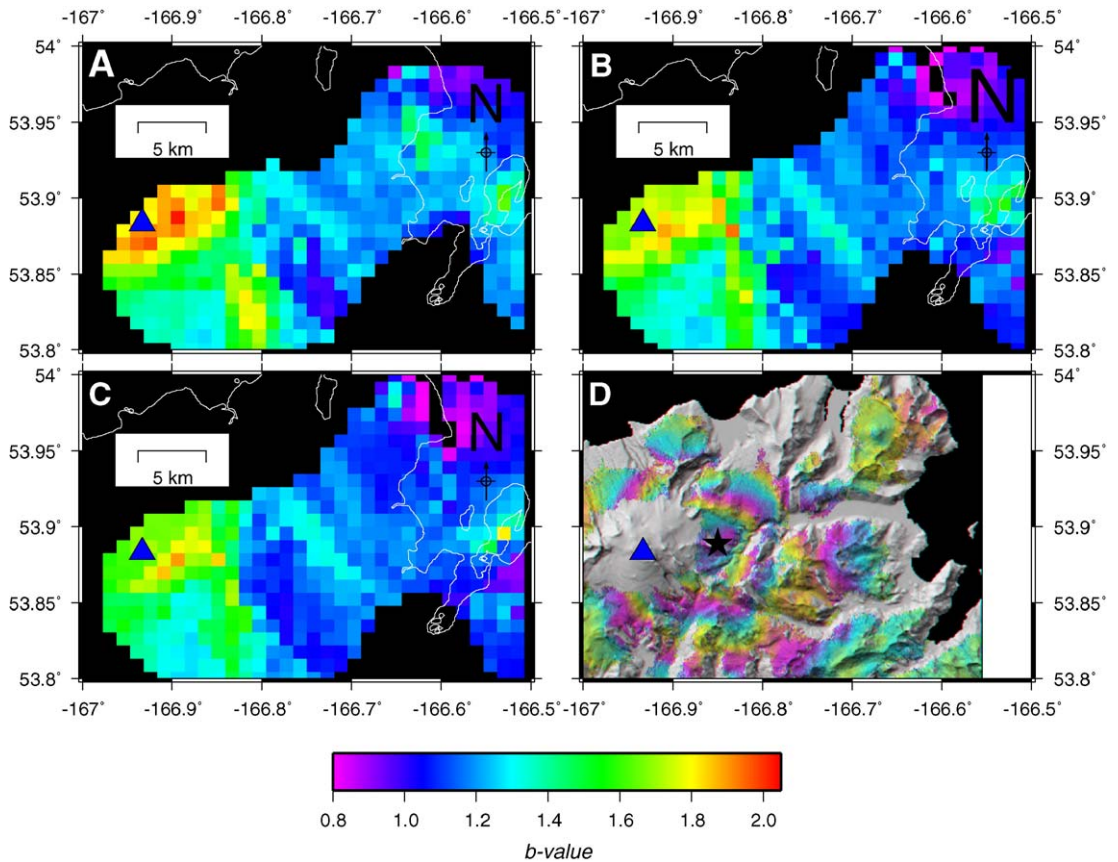


Fig. 3. A). Spatial distribution of b -values at 4 km depth. The black areas are areas with no data. The white line shows the coast of Unalaska. The blue triangle marks the main vent of Makushin. B). Spatial distribution of b -values at 6 km depth. C). Spatial distribution of b -values at 7 km depth. D). Result from Lu et al. [3] showing the ~ 7 cm uplift on Makushin's east flank. The center of the uplift is marked by the star. The white area to the right was not mapped in their study. Color scale at bottom is for parts A, B, and C. Colors in D indicate interferometric fringes.

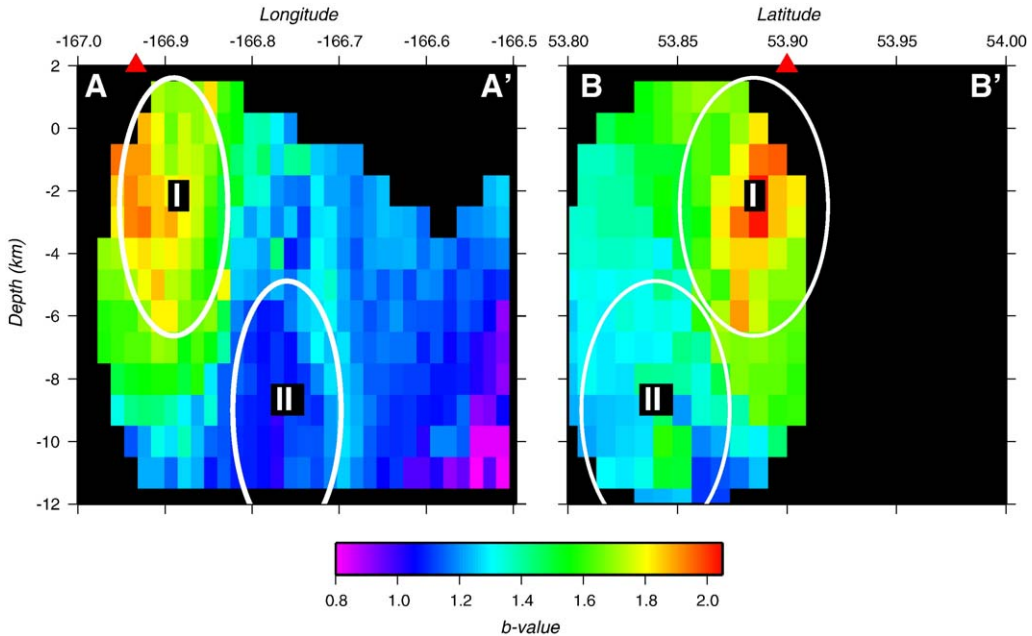


Fig. 4. Cross-sections, A–A' and B–B', of the study area (See Fig. 1 for locations). The red triangle marks the location of Maukusin's main vent. Area I is the high b -value anomaly to the east of main vent. Area II is the "normal" b -value area used as a comparison to area I. These are the areas used for Utsu's p -test.

The b -value for each node was calculated using the maximum likelihood (ML) method of Aki [35]:

$$b = \log e / (M_{\text{mean}} - M_o), \quad (3)$$

where M_{mean} is the mean magnitude and $M_o = M_c - 0.05$ (The width of magnitude bins used in our study is 0.1, so $0.1/2=0.05$). Using our algorithms and a catalog provided by Hoblitt et al. [36], we have successfully duplicated the spatial b -value pattern reported by Sanchez et al. [13] beneath Mt. Pinatubo, the Philippines. We also calculated b -values using least squares regression, and the spatial pattern remained generally unaffected.

4. Results

Measurements at a total of 5190 nodes were obtained. The overall average of the b -values for our study area is 1.21 with a range from 0.73 to 2.03 (Fig. 3). The range and magnitude of the observed b -values in the vicinity of Makushin are comparable with those from the other 13 volcanoes, beneath which b -values have been mapped [11].

As shown on the horizontal slices (Fig. 3), two areas with high b -values were detected. The primary anomaly

is located at about 4 km east of Makushin's main vent at a depth range of 4–7 km (Fig. 3). The other is found at about 7 km SE of the vent at approximately the same depth. We used the p -test [37] to quantify the statistical significance of the two anomalous areas.

We first calculate the p -value using

$$p = e^{(-dA/2-2)}, \quad (4)$$

where $dA = -2N \ln(N) + 2N_1 \ln(N_1 + N_2 b_1/b_2) + 2N_2 \ln(N_1 b_2/b_1 + N_2)$, N_1 and N_2 are the number of events in the similar spherical volumes to be compared, and $N = N_1 + N_2$. For the primary anomalous area (i.e., area I in Fig. 4), a sphere with a radius of 4 km is used, within which $N_1 = 29$ and the resulting b_1 is 1.84. For the background area (i.e., area II), $N_2 = 77$ and $b_2 = 1.12$. These values lead to a p of 0.012, suggesting that the probability that the two areas have the same b -values can be rejected at the 99% confidence limit [9]. We performed the same test for the second anomaly located at the SE of the main vent, and found that it is statistically insignificant, although it shows up independent of data processing parameters and techniques.

We next further test the robustness of the primary anomaly using several scenarios, some of which were used by previous studies (e.g., [13]). These include: (1) using a constant M_c for the whole study area, (2) varying

M_c , (3) using a fixed radius of 4 km and letting the number of events vary, (4) using different grid dimensions such as $1 \times 1 \times 2$ km, and (5) changing the number of samples N . The anomaly persistently exists in the resulting b -value spatial distributions, suggesting that the anomaly is a well-resolved real feature.

5. Discussion

Several factors can affect the reliability of the resulting b -value distribution, especially for volcanic areas. The first is the so-called nonlinearity of the FMD [38]. In volcanic areas, this is mostly due to the existence of a large number of earthquake swarms associated with magma movement [12]. The large number of small earthquakes in the swarms tend to increase the observed b -values and lead to a bimodal distribution in the FMD. Fortunately, such a nonlinear distribution is not observed in our catalog (see inset of Fig. 2B).

The second factor that can affect the results is the change in network coverage due to addition of new stations or station failures. This can create inconsistencies in magnitude reporting, which affect b -values. For the Makushin subnet, the only major change was the addition of station MREP on January 1, 2002. As can be observed in Fig. 2B, no large change in the rate of earthquake reporting occurred after MREP was added, indicating that the subnet was already operating at a reliable level before 2002.

Another factor is the limited number of recorded earthquakes in active volcanic zones. Depending on the volume to be mapped and the magnitude of the expected spatial variation in b -values, using a small number of events can lower the spatial resolution of the b -value map, and consequently reduce the robustness of the features identified [12]. The volume that we mapped, the magnitude of spatial variation in b -values, as well as the number of events are all comparable with a previous study conducted at Mt. Etna, Italy [17], which was considered as a successful example of b -value mapping in the vicinity of an active volcano [12]. In addition, the statistically significant anomaly, as suggested by the p -test, and the resulting physically reasonable b -value distribution indicate that the size of the catalog that we used is sufficient for the purpose of the study.

The primary anomaly is located in the vicinity of a magma chamber inferred from a recent InSAR study [3], which determined that a ~ 7 cm surface uplift occurred on Makushin's east flank between October 1993 and September 1995. The inferred magma chamber that was thought to be responsible for the uplift was centered ~ 5 km east of the volcano's summit at a depth of about

7 km below sea level (Fig. 3D). Inversion of the InSAR data suggested an increase of the magma chamber volume by 0.022 km^3 during the two-year period. This event occurred before the establishment of the Makushin subnet. Even though our seismic data are from 2001 to 2005, we detected a high b -value anomaly surrounding and above the magma chamber suggested by the InSAR data. The close correspondence can be explained by the existence of highly fractured rock located above and around the magma chamber, as a result of applied pressure from the expansion.

Another possible cause of the high b -value anomaly is vesiculation, i.e., release of magmatic gases due to pressure reduction at shallow (3–6 km) depth, as well as exsolution of gases. This mechanism has been suggested as being partially responsible for stress-induced rock fracturing above magma chambers [11,13], such as that found northwest of Pinatubo's vent [13]. Interaction between magma and groundwater and the consequent reduction of normal stress could also have contributed to the observed high b -values. Such a stress reduction allows for the occurrence of relatively more small earthquakes and thus increases the b -values [13].

The primary anomaly of high b -values is located about 4 km east of the vent rather than directly beneath it. This offset is similar to most other volcanoes studied so far, such as Mt. Etna in Italy, Mammoth in California, and Kilauea in Hawaii [12]. Complex rather than simple magma conduits were proposed as the cause of the observed offset [12]. Beneath Makushin, however, a simple model can be proposed to explain both the seismic and InSAR observations, that is, a recent expansion of a magma chamber located at about 4–5 km east of the main vent at ~ 7 km depth.

To our knowledge, this is the first time such a close spatial correspondence between b -value and InSAR observations has been made. Additional work will further enforce such a correspondence, and will deepen our understanding of the relationship between the surface uplift and the variations in the physical/chemical properties of the magma chamber and surrounding rocks.

Future seismic tomography studies can provide further information about the spatial distribution of the magma chamber(s) that might be responsible for the observed high b -value anomaly. Additional InSAR studies are necessary to address the question of whether the expansion happened again since 2000, which was the end of the InSAR data used by Lu et al. [3]. If the conclusion from the studies is that the expansion has ceased since September 1995, our seismic results may suggest that the healing process of the surrounding rocks affected by the magma expansion happened a decade

ago is still undergoing. This could provide some insight into the time scale of the thermal diffusion, which was considered as the main controlling factor for the long-term b -value anomalies after eruptions [11].

6. Conclusions

Using a seismic catalog of 491 events from July 2001 to April 2005, we created a spatial 3-D map of b -values under the Makushin Volcano, Unalaska Island, Alaska. A region of high b -values was found ~ 4 km east of Makushin's vent. Based on previous b -value studies of volcanoes and the spatial orientation of this anomaly, this feature is likely associated with a magma chamber located at ~ 7 km depth. The p -test and tests using different data processing parameters and techniques suggest that this is not an artifact of processing but a statistically significant anomaly.

Our findings are consistent with the results from a recent InSAR study [3], which found a ~ 7 cm uplift ~ 5 km east of Makushin's main vent. The proposed depth of ~ 7 km of a magma chamber coincides with our b -value variations. b -value mapping in conjunction with other geophysical techniques of locating magma chambers provides a way to improve our understanding of the active magmatic processes beneath a volcano.

Acknowledgments

We are grateful to James Dixon of AVO/USGS for providing the earthquake catalog used in the study. We would like to thank Steve McNutt for his useful insights and suggestions for the manuscript, Kelly Liu for the discussion, and two anonymous referees for the constructive reviews. The figures were produced using the Generic Mapping Tools [39]. This study was partially supported by the National Science Foundation under the awards EAR-0440320 and EAR-0207466.

References

- [1] J.E. Beget, C.J. Nye, K.W. Bean, Preliminary volcano-hazard assessment for Makushin Volcano, Alaska, Report of Investigation, 2004-4, Alaska Div. of Geol. and Geophys. Surv., Fairbanks, AK, 2000.
- [2] C.A. Neal, R.G. McGimsey, 1995 volcanic activity in Alaska and Kamchatka: summary of events and response of the Alaska Volcano Observatory, USGS Open-File Report, 96-0738, 1996, pp. 6–7.
- [3] Z. Lu, J.A. Power, V.S. McConnell, C. Wicks Jr., D. Dzuris, Preeruptive inflation and surface interferometric coherence characteristics by satellite radar interferometry at Makushin volcano, Alaska: 1993–2000, *J. Geophys. Res.* 107 (2002) 2266, doi:10.1029/2001JB000970.
- [4] M. Ishimoto, K. Iida, Observations of earthquakes registered with the microseismograph constructed recently, *Bull. Earthquake Res. Inst., Univ. Tokyo* 17 (1939) 443–478.
- [5] B. Gutenberg, C.F. Richter, Frequency of earthquakes in California, *Bull. Seismol. Soc. Am.* 34 (1944) 185–188.
- [6] K. Mogi, Magnitude–frequency relation for elastic shocks accompanying fractures of various materials and some related problems in earthquakes, *Bull. Earthquake Res. Inst., Univ. Tokyo* 40 (1962) 831–853.
- [7] C.H. Scholz, The frequency–magnitude relation of microfracturing in rock and its relation to earthquakes, *Bull. Seismol. Soc. Am.* 58 (1968) 399–415.
- [8] A. Udas, *Principles of Seismology*, Cambridge University Press, New York, 1999.
- [9] M.K. Wyss, K. Shimazaki, S. Wiemer, Mapping active magma chambers beneath the off-Ito volcano, Japan, *J. Geophys. Res.* 102 (1997) 413–420.
- [10] C. Frolich, S. Davis, Teleseismic b -values: or much ado about 1.0, *J. Geophys. Res.* 98 (1993) 631–644.
- [11] S.R. McNutt, Volcanic seismology, *Annu. Rev. Earth Planet. Sci.* 32 (2005) 461–491.
- [12] S. Wiemer, M. Wyss, Mapping spatial variability of the frequency–magnitude distribution of earthquakes, in: Dmowska (Ed.), *Advances in Geophysics*, vol. 43, 2002, 336 pp.
- [13] J.J. Sanchez, S.R. McNutt, M. Wyss, Spatial variations in the frequency–magnitude distribution of earthquakes at Mount Pinatubo Volcano, *Bull. Seismol. Soc. Am.* 94 (2004) 430–438.
- [14] S. Wiemer, S.R. McNutt, Variations in the frequency–magnitude distribution with depth in two volcanic areas: Mount St. Helens, Washington, and Mount Spurr, Alaska, *Geophys. Res. Lett.* 24 (1997) 189–192.
- [15] S. Wiemer, S.R. McNutt, M. Wyss, Temporal and three dimensional spatial analysis of the frequency–magnitude distribution near Long Valley caldera, California, *Geophys. J. Int.* 134 (1998) 409–421.
- [16] M.F. Wyss, F. Klein, K. Nagamine, S. Wiemer, Anomalously high b -values in the south flank of Kilauea Volcano, Hawaii: evidence for the distribution of magma below Kilauea's east rift zone, *J. Volcanol. Geotherm. Res.* 106 (2001) 23–37.
- [17] M. Murru, C. Montuori, M. Wyss, E. Privitera, The locations of magma chambers at Mt. Etna, Italy, mapped by b -values, *Geophys. Res. Lett.* 26 (1999) 2553–2556.
- [18] J.S. Power, M. Wyss, M.J. Latchman, Spatial variations in the frequency–magnitude distribution of earthquakes at Soufriere Hills volcano, Montserrat/West Indies, *Geophys. Res. Lett.* 25 (1998) 3653–3656.
- [19] J. Mori, D. Eberhart-Phillips, D.H. Harlow, Three Dimensional velocity structure at Mount Pinatubo: resolving magma bodies and earthquake hypocenters, in: C.G. Newhall, R.S. Punongbayan (Eds.), *Fire and Mud: Eruptions and Lahars of Mt. Pinatubo*, Philippines, PHIVOLCS and University of Washington, Seattle, 1996, pp. 371–382.
- [20] J.M. Lees, The magma system of Mount St. Helens: nonlinear high-resolution P -wave tomography, *J. Volcanol. Geotherm. Res.* 53 (1992) 103–116.
- [21] C. Widiwijayanti, A. Clarke, D. Elsworth, B. Voight, Geodetic constraints on the shallow magma system at Soufriere Hills Volcano, Montserrat, *Geophys. Res. Lett.* 32 (2005) L11309, doi:10.1029/2005GL022846.
- [22] D. Patane, P. De Gori, C. Chiarabba, A. Bonaccorso, Magma ascent and the pressurization of Mt. Etna's volcanic system, *Science* 299 (2003) 2061–2063.

- [23] N.W. Warren, G.V. Latham, An experimental study of thermally induced microfracturing and its relation to volcanic seismicity, *J. Geophys. Res.* 75 (1970) 4455–4464.
- [24] M. Wyss, Towards a physical understanding of the frequency–magnitude distribution, *Geophys. J. R. Astron. Soc.* 31 (1973) 341–359.
- [25] J.P. Dixon, S.D. Stihler, J.A. Power, G. Tytgat, S.C. Moran, J.J. Sanchez, S.R. McNutt, S. Estes, J. Paskievitch, Catalog of earthquake hypocenters at Alaskan volcanoes: January 1 through December 31, 2003, USGS Open-File Report 2004-1234, 2004.
- [26] J.C. Lahr, HYPOELLISE: a computer program for determining local earthquake hypocentral parameters, magnitude, and first-motion pattern, USGS Open-File Report 99-23, 1999.
- [27] J.P. Dixon, S.D. Stihler, J.A. Power, G. Tytgat, S.C. Moran, J.J. Sanchez, S.R. McNutt, S. Estes, J. Paskievitch, Catalog of earthquake hypocenters at Alaskan volcanoes: January 1 through December 31, 2002, USGS Open-File Report 2003-0267, 2003.
- [28] J.P. Dixon, S.D. Stihler, J.A. Power, G. Tytgat, S. Estes, S.C. Moran, J. Paskievitch, S.R. McNutt, Catalog of earthquake hypocenters at Alaskan volcanoes: January 1, 2000 through December 31, 2001, USGS Open-File Report 2002-0342, 2002.
- [29] A.D. Jolly, S.D. Stihler, J.A. Power, J.C. Lahr, J. Paskievitch, G. Tytgat, S. Estes, A.B. Lockhart, S.C. Moran, S.R. McNutt, W.R. Hammond, Catalog of earthquake hypocenters at Alaskan volcanoes: January 1, 1994 through December 31, 1999, USGS Open-File Report 2001-0189, 2001.
- [30] A.M. Cao, S.S. Gao, Temporal variation of seismic *b*-values beneath northeastern Japan island arc, *Geophys. Res. Lett.* 29 (2002), doi:10.1029/2001GL013775.
- [31] Y. Ogata, K. Katsura, Analysis of temporal and spatial heterogeneity of magnitude frequency distribution inferred from earthquake catalogs, *Geophys. J. Int.* 113 (1993) 727–738.
- [32] S. Wiemer, M. Wyss, Minimum magnitude of completeness in earthquake catalogs: examples from Alaska, the Western United States, and Japan, *Bull. Seismol. Soc. Am.* 90 (2000) 859–869.
- [33] J. Woessner, S. Wiemer, Assessing the quality of earthquake catalogs: estimating the magnitude of completeness and its uncertainty, *Bull. Seismol. Soc. Am.* 95 (2005) 684–698.
- [34] S. Wiemer, J. Benoit, Mapping the *b*-value anomaly at 100 km depth in Alaska and New Zealand subduction zones, *Geophys. Res. Lett.* 23 (1996) 1557–1560.
- [35] K. Aki, Maximum likelihood estimate of *b* in the formula $N=a-bM$ and its confidence limits, *Bull. Earthquake Res. Inst., Univ. Tokyo* 43 (1965) 237–239.
- [36] R.P. Hoblitt, J. Mori, J.A. Power, Computer visualization of earthquake hypocenters, in: C.G. Newhall, R.S. Punongbayan (Eds.), *Fire and Mud: Eruptions and Lahars of Mt. Pinatubo, Philippines*, PHIVOLCS and University of Washington, Seattle, 1996, pp. 383–385.
- [37] T. Utsu, On seismicity, *Report of the Joint Research Institute for Statistical Mathematics*, Tokyo, 1992, pp. 139–157.
- [38] L. Knopoff, The magnitude distribution of declustered earthquakes in Southern California, *Proc. Natl. Acad. Sci. U. S. A.* 97 (2000) 11,880–11,884.
- [39] P. Wessel, W.H.F. Smith, Free software helps map and display data, *EOS Trans. AGU*, vol. 72, 1991, p. 441.